NASA Contractor Report 165596

FAST GENERATION OF THREE-DIMENSIONAL COMPUTATIONAL BOUNDARY-CONFORMING PERIODIC GRIDS OF C-TYPE

Djordje S. Dulikravich

Universities Space Research Association
Columbia, Maryland 21044

June 1982

Prepared for

NATIONAL AERONAUTICS AND SPACE ADMINISTRATION
Lewis Research Center
Under Contract NAS3-22532

FAST GENERATION OF THREE-DIMENSIONAL COMPUTATIONAL BOUNDARY-CONFORMING PERIODIC GRIDS OF C-TYPE

Djordje S. Dulikravich*
Universities Space Research Association
Columbia, Maryland 21044

ABSTRACT

A fast computer program, GRID3C, has been developed to generate multilevel three-dimensional, C-type, periodic, boundary conforming grids for the calculation of realistic turbomachinery and propeller flow fields. The technique is based on two analytic functions that conformally map a cascade of semi-infinite slits to a cascade of doubly infinite strips on different Riemann sheets. Up to four consecutively refined three-dimensional grids can be automatically generated and permanently stored on four different computer tapes. Grid nonorthogonality is introduced by a separate coordinate shearing and stretching performed in each of three coordinate directions. The grids can be easily clustered closer to the blade surface, the trailing and leading edges and the nub or shroud regions by changing appropriate input parameters. Hub and duct (or outer free boundary) can have different axisymmetric shapes. A vortex sheet of arbitrary thickness emanating smoothly from the blade trailing edge is generated automatically by GRID3C. Blade cross-sectional shape, chord length, twist angle, sweep angle, and dihedral angle can vary in an arbitrary smooth fashion in the spanwise direction. Input coordinates must be Cartesian, while the output grid coordinates can be Cartesian or cylindrical.

INTRODUCTION

When numerically solving partial differential equations governing the flow of fluid through realistically shaped configurations, exact boundary conditions must be applied at correct locations. This is especially important when calculating internal flows and flows that are governed by nonlinear partial differential equations. Seemingly negligible alterations of geometrical shape or flow conditions at the boundary can drastically change the basic features of the flow field, for example, choking an originally unchoked flow or changing a shock-free flow into a shocked flow[1]. The most economical and accu-

---

*Presently Assistant Professor of Aerospace Engineering and Engineering Mechanics, The University of Texas at Austin.

rate way to numerically apply exact boundary conditions on solid boundaries is to generate and use a computational grid that conforms to these surfaces (fig. 1). Recent numerical techniques do not require orthogonal grids[2] because they use locally isoparametric formulation when numerically determining derivatives of geometric and flow variables. A widely accepted procedure for accelerating an iterative solution process of the flow equations and for resolving or capturing high flow gradients is to perform calculations on a sequence of several successively refined grids. The multigrid technique[3] usually requires four to six such grids. For realistic threedimensional configurations the number of grid points to be generated is prohibitively large even for inviscid flow calculations. Computational grids for such configurations should be easy to regenerate if shock waves and vortex sheets are to be better resolved or if the configuration of the solid boundaries changes with time.

An H-type grid (fig. 1) provides excellent resolution of the flow field at upstream and downstream infinity. It is also the simplest grid to generate. At the same time, H-type grid does not provide for an accurate treatment of rounded leading and trailing edges and wastes points in the flow domains away from the boundaries. An O-type grid represents the other extreme. It gives a very poor resolution at infinities[4], thus creating a problem when Cauchy-type boundary conditions must be enforced at the supersonic inflow boundary (fig. 2). A grid of the O-type also does not provide desirable resolution in the vicinity of the vortex sheet. An open trailing edge simulation of the boundary layer displacement thickness effect cannot be readily incorporated. Nevertheless, an O-type grid provides for accurate discretization of arbitrarily blunt leading and trailing edges and requires a minimum number of grid points. A combination of an O-type grid in the upstream region and an H-type grid in the downstream region creates a C-type grid. This type of grid provides for a good treatment of all boundary and periodicity conditions including wake treatment and supersonic exit flow, although it lacks an adequate resolution at upstream infinity (fig. 1).

In turbomachinery and rotorcraft flow field calculations the flow field is periodic and a geometrically periodic grid provides for a simple and accurate way to enforce the flow periodicity. The simplest and fastest way to generate nonorthogonal periodic grids is to avoid time-consuming techniques based on the numerical solution of sets of partial differential equations whenever possible. Instead, a basic knowledge of complex variables and conformal mapping can be used together with a few additional nonorthogonal coordinate shearings and stretchings. A three-dimensional, periodic, O-type grid generator code was already developed[4] by using this technique, which guarantees that the

grid lines of the same family do not intersect because the basis of the technique is conformal mapping. Another view of a three-dimensional, periodic O-type grid is presented in figure 3.

The Computational Fluid Mechanics Branch of the NASA Lewis Research Center provided computational Facilities used in this work. Dr. Charles Putt of NASA Lewis Computer Services Division, Dr. Bharat Soni of Sverdrup Technology, Inc., and Mr. William Usab of MIT and United Technologies Research Center exercised the computer codes and provided several grid displays.

SHEARING AND STRETCHING IN PHYSICAL SPACE

Conformal mapping can be applied only to two-dimensional plane surface problems. A general procedure for creating such planes can be best described in the case of a rotor mounted on a hub shaped like a doubly infinite circular cylinder and confined inside a doubly infinite circular-cylinder-shaped duct. The intermediate doubly infinite circular-cylinder-shaped surfaces intersecting the blades can be viewed as planes when expressed in terms of $(x,r\theta)$ coordinates. A standard procedure for creating three-dimensional blade shapes is to specify local airfoil shapes on a number of input planes that are orthogonal to a straight radial line. This radial line (z axis in fig. 4) is called a stacking axis, and local blade sweep and dihedral angles are measured from that line (fig. 1). Input planes are defined by z = constant. Intermediate cylindrical surfaces, which we seek for the next step in this grid generation procedure are defined by r = constant. To obtain an intersection contour between the blade surface and r = constant cylindrical surfaces, a spline fitting and interpolation procedure is used along the blade. Input airfoil (x_i,y_i) coordinates on z = constant planes are transformed into cylindrical coordinates

$$x = x_i \tag{1}$$

$$\theta = \arctan(y_i/z_i) \tag{2}$$

$$r = (y_i^2 + z_i^2)^{1/2} \tag{3}$$

Cylindrical coordinates $(x,r\theta)$ are interpolated at r = constant spanwise locations, thus defining blade cross sections on r = constant cylindrical surfaces.

On the other hand, realistically shaped hubs and ducts are not doubly infinite circular cylinders but axisymmetric surfaces. Therefore, the intermediate surfaces are also axisymmetric and not cylindrical. Nevertheless, the

same grid generation technique can be used if a simple nonorthogonal shearing (or normalization) and stretching of the radial coordinate (fig. 3) is performed. Nonorthogonal (unidirectional) shearing of the r coordinate converts the axisymmetric surfaces into cylindrical surfaces defined by R = constant. Let subscripts H,T, and D designate R = constant surfaces corresponding to hub,blade tip, and duct (or outer free boundary) location, respectively. Also let the normalized radial coordinate be defined as

$$\bar{R} = \frac{r(x_i) - r_H(x_i)}{r_D(x_i) - r_H(x_i)} \tag{4}$$

The radial coordinate in the hub-to-tip region is stretched and sheared with the following function

$$R = R_H + (R_T - R_H)((\bar{R}/\bar{R}_T) + A \sin(2\pi\, \bar{R}/\bar{R}_T)) \tag{5}$$

The following value was obtained from experience

$$R_H = N/50.0 \tag{6}$$

The stretching parameter, A, gives best results if

$$0.12 > A > 0.0 \tag{7}$$

When A = 0, the cylindrical cutting surfaces R = constant are equidistantly spaced from hub to tip. Let the normalized, sheared radial coordinate in the region between the blade tip and the duct (or outer radial boundary) surface be

$$\overset{*}{R} = (\bar{R} - \bar{R}_T)/(\bar{R}_D - \bar{R}_T) \tag{8}$$

The stretching function for the tip-to-duct domain is chosen to be

$$R = 1.0 + (R_H - q)\overset{*}{R} + q\,\overset{*2}{R} \tag{9}$$

This function must have the same slope, q, at the location R = 1 as the stretching function in the domain between the hub and the tip (eq. 5).

$$q = (1 + A)(1 - R_H)/R_T \tag{10}$$

Combining the two stretching functions (eqs. 5 and 9) provides for a smooth and continuous transformation from the physical r coordinate into the sheared R coordinate (fig. 4). For a stator or rotor with no tip clearance, equation 9 is not needed.

Frequently, the input points are not clustered in the same regions on each input plane. Moreover, the number of input points defining the blade cross section on each input plane can vary from one input plane to the next. To accurately determine intersection contours between the blade surface and the axisymmetric surfaces, the corresponding input points must be located at the same percentage of the blade chord length on each input plane. Implicitly, this means that the number of input points must be the same on all input planes. Therefore, these input points must be appropriately redistributed on each input plane. This redistribution can be performed with respect to the input airfoil contour coordinate defined as

$$s = [(x_i - x_{i-1})^2 + (y_i - y_{i-1})^2]^{1/2} \qquad (11)$$

Then the input Cartesian coordinates can be expressed in terms of the input airfoil contour coordinates. Coordinate s is measured clockwise around the input airfoil contour, starting and ending at the trailing edge point. As it was stated earlier, the number of contour points on the pressure surface must be the same as the number of contour points on the suction surface. For non-symmetric airfoils the lengths of these two contour lines are generally not the same. Let ITS denote the trailing edge point on the suction side and ITP denote the trailing edge point on the pressure side of the input airfoil. Also, let LE denote the leading edge, that is, the point that is farthest from the trailing edge. The normalized surface coordinate is defined as

$$\bar{S} = \frac{s - s_{ITP}}{s_{LE} - s_{ITP}} \qquad (12)$$

The redestribution of input points is performed with the following stretching function

$$\bar{S}^* = (1 - \bar{S})\bar{S}^B + \bar{S}[1 - (1 - \bar{S})^B] \qquad (13)$$

where the exponent B should satisfy

$$1.4 > B > 1.0 \qquad (14)$$

When B = 1 the points are equidistantly spaced along the airfoil contour. The points along the pressure surface are redistributed by using the formula

$$S = \bar{S}^*(s_{LE} - s_{ITP}) \qquad (15)$$

and the points along the suction surface are redistributed by using the formula

$$S = \overset{*}{S}(s_{ITS} - s_{LE}) + (s_{LE} - s_{ITP}) \qquad (16)$$

This redistribution of input coordinates x and y is performed with a cubic spline fitting applied in the s direction. Interpolation is performed at S locations. Spline fitting and interpolation are also used with respect to the R coordinate in order to find the points on intersection contours between the blade surface and the intermediate axisymmetric surfaces. Locations of those points in the physical space will not be altered with the subsequent mapping-remapping procedure.

The exact shape of the wake of arbitrary thickness is not known a priori. To eliminate the need for specifying the location of the wake in the preparation of the input, the shape of the wake centerline is automatically generated by using the simple polynomial expression

$$y = a(x - x_{TE})^3 + b(x - x_{TE})^2 + c(x - x_{TE}) + y_{TE} \qquad (17)$$

Here the trailing edge point coordinates are

$$x_{TE} = (x_{ITP} + x_{ITS})/2 \qquad (18)$$

and

$$y_{TE} = (y_{ITP} + y_{ITS})/2 \qquad (19)$$

The point where the wake centerline intersects the downstream-infinity cutoff boundary is defined with the subscript EX. Let c be the average slope of the pressure and suction surfaces of the airfoil at the trailing edge , and let d be the slope of the expected flow angle at the exit boundary. Then the constants a and b in equation 17 are

$$a = [x_w(c + d) - 2\, y_w]/x_w^3 \qquad (20)$$

and

$$b = [3y_w - x_w\,(2c + d)]/x_w^2 \qquad (21)$$

where

$$x_w = x_{EX} - x_{TE} \qquad (22)$$

and

$$y_w = y_{EX} - y_{TE} \tag{23}$$

Wake surface grid points are redistributed (stretched) with the formula

$$x^* = (x - x_{TE})/x_w - n \sin(\pi(x - x_{TE})/x_w) \tag{24}$$

The stretching exponent, n, is determined from the continuity of the slope of the stretching functions at the trailing edge (eqs. 13, 15, 16, 22, and 24)

$$n = 1.05(1.0 - B/2x_w)/\pi \tag{25}$$

If the wake has a finite thickness, that is, if the blade trailing edge is open, coordinates of the points on the upper and lower surfaces of the wake are determined by adding and subtracting the trailing edge half thickness. The axial coordinate of the upper surface of the wake is determined from the formula

$$x^u = x + (x_{ITS} - x_{ITP})/2 \tag{26}$$

and that of the lower surface of the wake by the formula

$$x^l = x - (x_{ITS} - x_{ITP})/2 \tag{27}$$

with similar expressions for the y coordinate. Superscripts u and l designate the upper and lower surfaces of the wake, respectively.

CONFORMAL MAPPING AND REMAPPING

The conformal mapping portion of the present procedure for generating three-dimensional, periodic C-type grids was originally used by Sockol to generate orthogonal, two-dimensional, cascade C-type grids. If the blades are straight, semiinfinite twisted plates of zero thickness, their intersections with circular cylinders generates doubly infinite cascades of semi-infinite straight slits on each of the (x,Rθ) planes (fig. 5). Each of these R = constant planes can be defined in terms of complex variables

$$w = x + iR\theta \tag{28}$$

The goal is to generate a boundary-conforming, periodic C-type grid on each of

the planes. This task is accomplished by conformally mapping the w plane via an intermediate "circle" complex plane (fig. 6)

$$v = \xi + i\eta \tag{29}$$

into the interior of a "doubly infinite strip" plane (fig. 7)

$$u = X + iY \tag{30}$$

Uniform grid in the u plane is then conformally remapped into the w plane, thus generating the desired C-type grid. As shown by Sockol[4] a single analytic function

$$w = w_{LE} + e^{\beta} \frac{R}{N}(2\beta \sin\beta + 2\cos\beta \ln(2\cos\beta)) - e^{-i\beta}(\ln v - i\pi) - 2\cos\beta \ln(1 - v) \tag{31}$$

where N is the number of blades and β is the local stagger angle on the R = constant surface, conformally maps the interior of the unit circle in the v plane to the interior of a periodic strip enveloping a semi-infinite slit in the w plane. The center of the circle (v = 0) maps into upstream infinity in the w plane and the point v = -1 maps into downstream infinity in the w plane. The zero-thickness slit between the points v = 0 and v = -1 maps into the upper and lower periodic boundary of a periodic strip in the w plane. The circle in the v plane maps into a semi-infinite straight slit in the w plane. A doubly infinite cascade of semi-infinite straight slits in the w plane is thus created by conformally mapping a doubly infinite cascade of Riemann sheets (v planes) that are interconnected through the slits between the points v = 0 and v = -1. Sockol[4] used a simple analytic function

$$v = \tanh(u^2/2) \tag{32}$$

to conformally map the interior of a doubly infinite straight strip in the u plane into the interior of a unit circle in the v plane. The lower strip boundary ($Y = -i\pi/2$) in the u plane maps into the circle in the v plane. The upper strip boundary (Y = 0) maps into a zero-thickness slit between the points v = 0 and v = -1. Axial infinities ($X = \pm\infty$) map into a single point (v = -1). The origin (X = 0; Y = 0) in the u plane maps into the origin (v = 0) in the v plane.

Realistically shaped blade airfoils are not straight semi-infinite lines of zero thickness. A C-type grid generated with the use of equations 31 and 32 alone will not conform to the actual airfoil cascade shapes on R = constant surfaces. To generate a C-type grid that conforms to the shape of the airfoil and wake , several nonorthogonal coordinate shearings and stretchings are used. Airfoil surface points are conformally mapped from the w plane via the v plane into the u plane. As a result, the circle in the v plane becomes deformed (fig. 7), and the corresponding lower wall in the u plane becomes an irregular line (fig. 8). The inverse of equation 31 cannot be analytically obtained for staggered cascades. Therefore, a Newton-Raphson procedure is used to iteratively evaluate on a point-by-point basis the pairs of (ξ,η) coordinates corresponding to the given pairs of $(x,R\theta)$ coordinates. By using an analytic inverse of equation 32, that is,

$$u = \left[\ln\left(\frac{1+v}{1-v}\right)\right]^{1/2} \qquad (33)$$

the deformed circle is conformally mapped from the v plane into the u plane.

SHEARING AND STRETCHING IN COMPUTATIONAL SPACE

It should be pointed out that with the increase in stagger angle in the w plane the image of the leading edge point shifts along the deformed circle in the v plane and along the deformed lower boundary in the u plane. To insure that the corresponding points along the periodic boundaries in the w plane have the common values of x coordinate, their images in the u plane are placed symmetrically along the Y = 0 line (fig. 9). At the same time these periodic points are distributed with a simple stretching function

$$X^U = X^U - e \sin(2\pi X^U/(X^L_{ITS} - X^L_{ITP})) \qquad (34)$$

Superscript U denotes the upper wall (Y = 0) of the u plane and superscript L denotes the lower irregular boundary of the u plane. The stretching coefficient e is determined from experience as

$$e = 0.18 - 0.05 \ln(2R\pi/Nt) \qquad (35)$$

where t is the local blade chord. The periodic grid points located in the wake region are redistributed by using the expression

$$X^U = X^U - f \sin(2\pi(|X|^U - X^U_{ITS})/(X^L_{MAXXP} - X^U_{ITS})) \quad (36)$$

where MAXXP denotes the last point on the upper surface of the wake. The stretching coefficient, f, is determined also from the experience as

$$0.10 > f > 0.05 \quad (37)$$

Because only a finite length of the wake is conformally mapped from the w plane into the u plane, the deformed strip in the u plane has a finite length. The shape of the end wall boundaries in the u plane are determined so that they meet the lower boundary of the strip in the u plane almost orthogonally (fig. 8). Consequently, grid orthogonality is well preserved at the wake. Coordinates of the grid points inside the strip in the u plane are determined from

$$Y = Y^L((Y/Y^L) + g \sin(\pi Y/Y^L)) \quad (38)$$

and

$$X = X^U + (X^L - X^U)\,((Y/Y^L) + C \sin(\pi Y/Y^L)) \quad (39)$$

where

$$0.30 > C > 0.15 \quad (40)$$

$$g = C\,(1.0 - 1.0/\cosh h) \quad (41)$$

$$h = 5\,(X^U/X^U_{MAXXP}) \quad (42)$$

Stretching coefficients C, g, and h are determined from experience and from the condition that C-type grid lines in the w plane closely follow the wake contour. Larger values of C generate grids suitable for viscous flow calculations, because grid layers are positioned closer to the blade and wake surface.

The resulting two-dimensional nonorthogonal periodic grid in the u plane is conformally mapped back into the w plane on a point-by-point basis. Finally, determination of the physical r coordinates of the grid points on the (x,Rθ) planes is obtained by reshearing the R coordinate (eqs. 4, 5, 8, and 9) and fitting it with respect to the x coordinate with a cubic spline.

RESULTS

On the basis of the preceding analysis, a computer program GRID3C was developed and tested[6]. Program GRID3C consists of 1150 card statements and requires approximately 500 K of computer memory Because of the analytical character of most of the transformations used, GRID3C is very fast. To generate and permanently store x,y,z coordinates of a typical four-level grid sequence consisting of (33*8*6),(63*13*11),(123*23*21),(243*43*41) grid points, respectively, GRID3C requires between three and four minutes of CPU time on an IBM 370/3033 computer. The Newton-Raphson iterative point-by-point mapping procedure of the airfoil and wake contour from the w plane into the v plane consumes most of the computer time. But this procedure needs to be performed only once on each axisymmetric surface.

Input to GRID3C must be provided in the x,y,z coordinate system, while the output grid coordinates can be computed in the x,y,z or x,r,θ coordinate system. GRID3C can automatically generate up to four successively refined three-dimensional grids and store them on four separate tapes. Computational grids for the blades with closed trailing edge (fig. 10) and for the blades with open trailing edge (fig. 11) can be generated with GRID3C code. For repetitive runs with different numbers of blades or different blade setting angles, only one input parameter needs to be changed in the input deck. Clustering of grid points closer to the leading and trailing edges and closer to the blade and vortex sheet surface (fig. 12) can be easily achieved by varying coordinate stretching parameters A, B, and C. Grid nonorthogonality is almost entirely removed from the airfoil and wake surface. Nevertheless, grid nonorthogonality can become intolerable if this grid generation technique is applied to closely spaced, highly staggered and cambered blades. Nonorthogonality can become excessive in the leading edge region of any blade if the end point of the semi-infinite slit in the w plane is not positioned approximately midway between the leading edge and its center of curvature.

An unsatisfactory grid resolution inherent to the C-type grids can be observed in figure 13. This figure shows a rectangular wing - cylindrical fuselage combination and two computational grid surfaces: one corresponding to the surface of the fuselage and the other being an intermediate surface located between the hub and the wing tip. Note that the wing extension beyond the tip has linearly increasing cord length. The GRI3C code automatically calculates wing (or blade) chord lengths at the off-tip locations based on the constraint

that gap-to-chord ratio at the tip should be retained at all outer spanwise locations. Key elements of a three-dimensional C-type grid generated by the GRID3C code for an advanced, eight-blade, transonic, NASA propeller is presented in figures 14 and 15 with intersection contours between a blade and the axisymmetric sur- faces shown. Note the large twist, sweep, and taper variations and the fact that the propeller hub is axisymmetric.

With minor modifications GRID3C can be used for generating computational grids applicable to a midmounted wing-body combination or a finned missile in free air or inside a wind tunnel having axisymmetric walls.

REFERENCES

1. Dulikravich, D.S.and Sobieczky, H., "Shockless Design and Analysis of Transonic Blade Shapes," AIAA Paper 81-1237; also NASA TM-82611, 1981.
2. Dulikravich, D.S., " Numerical Calculation of Inviscid Transonic Flow Through Rotors and Fans," Ph.D.Thesis, January 1979.(available through University Microfilms International, 300 N.Zeeb Road, Ann Arbor, MI 48106)
3. Jameson, A., "Acceleration of Transonic Potential Flow Calculations on Arbitrary Meshes by the Multiple Grid Method," AIAA 4th Computational Fluid Dynamics Conference, July 23-25, 1979, Williamsburg, Va., pp.122-146.
4. Numerical Grid Generation Techniques, NASA CP-2166, 1980.
5. Dulikravich, D.S., "GRID3O-Computer Program for Fast Generation of Multi-level, Three-Dimensional, O-type Boundary Conforming Computational Grids," NASA TP-1920, 1981.
6. Dulikravich, D.S., "GRID3C-Computer Program for Generation of C-Type, Three-Dimensional, Boundary-Conforming, Periodic Grids," NASA CR-167846, 1982.

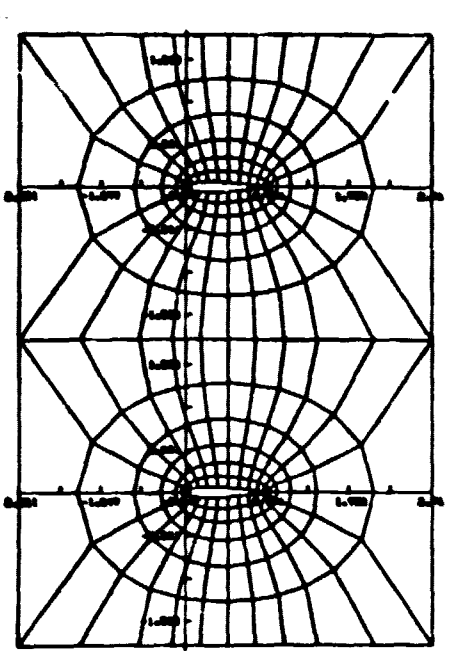

O-TYPE GRID

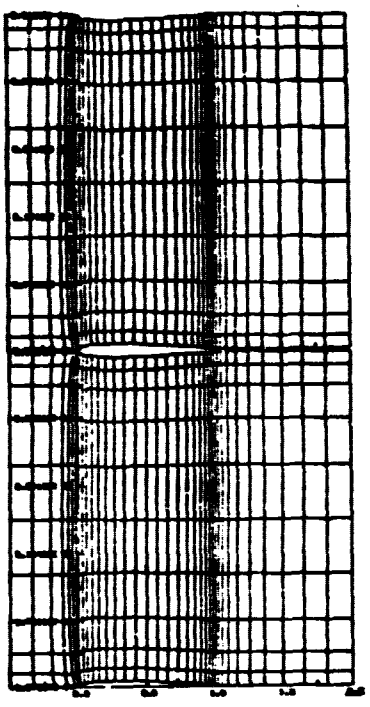

H-TYPE GRID

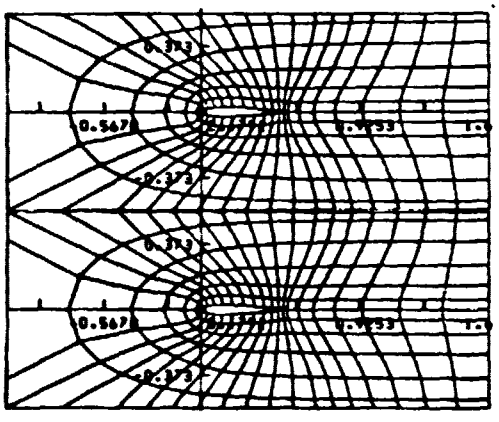

C-TYPE GRID

Figure 1. - Three basic types of two-dimensional, conforming, computational grids.

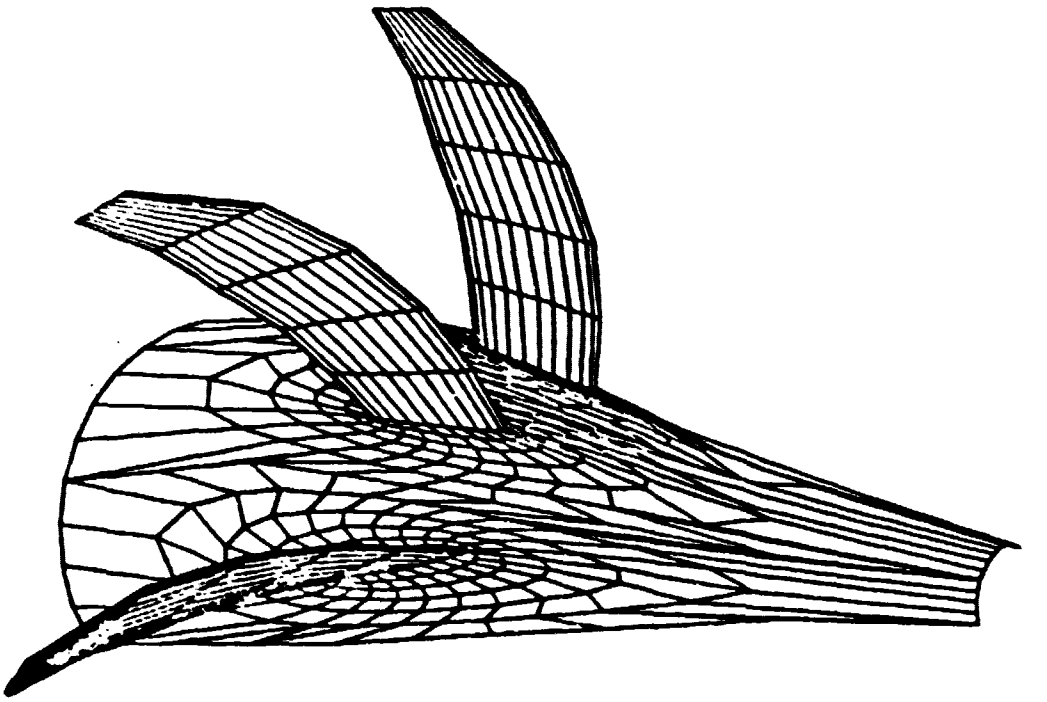

Figure 2. - Axisymmetric view of a three-dimensional, O-type, periodic boundary conforming grid for NASA eight-blade transonic prop fan. Shown are the hub surface grid and three neighboring blades with their surface grids.

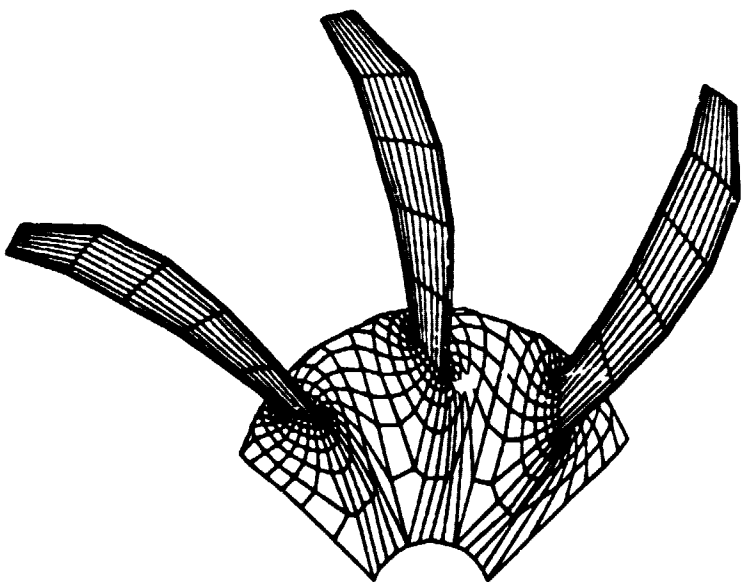

Figure 3. - Frontal view of the O-type grid for NASA eight-blade transonic prop fan.

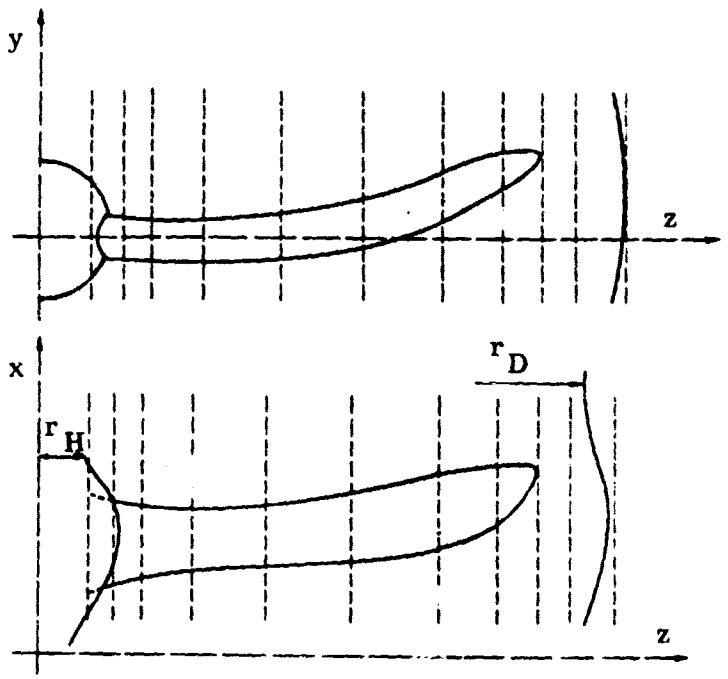

Figure 4. - Spanwise input planes (stations) perpendicular to the stacking (z) axis. Physical x,y,z coordinate system rotates with the blade.

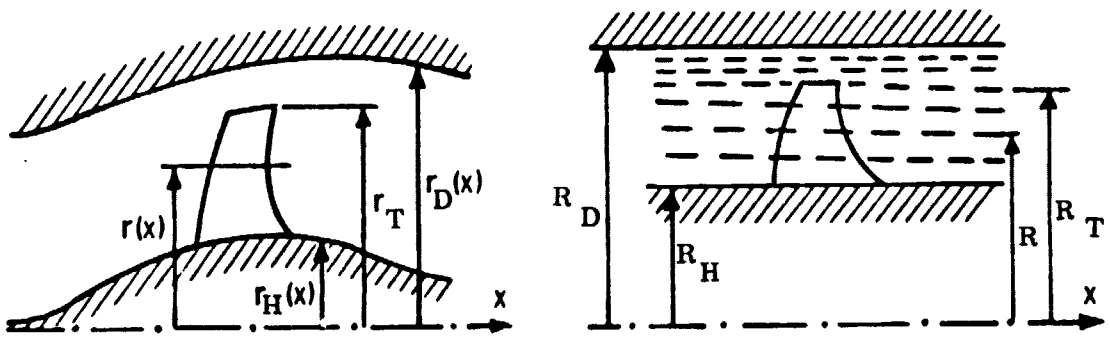

Figure 5. - Radial coordinate nonorthogonal sheering concept.

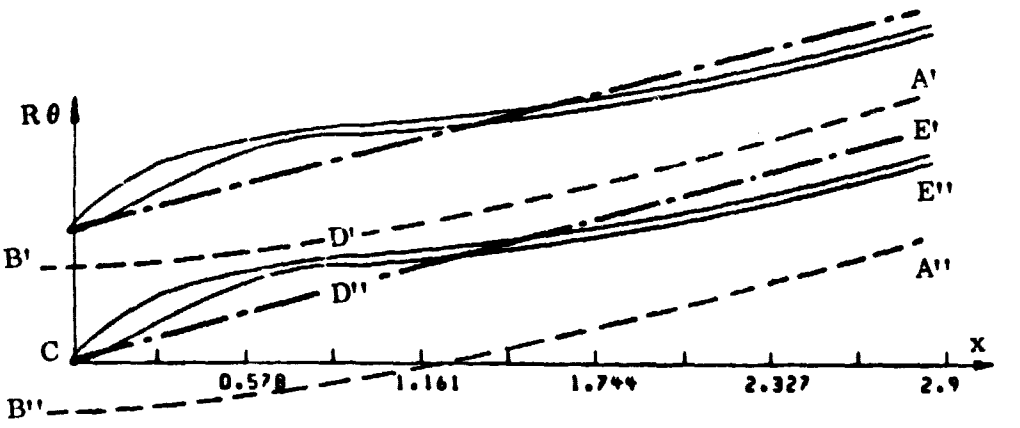

Figure 6. - Two-dimensional cascade of semi-infinite staggered slots of zero thickness with an indication of a cascade of realistically shaped airfoils and their wakes.

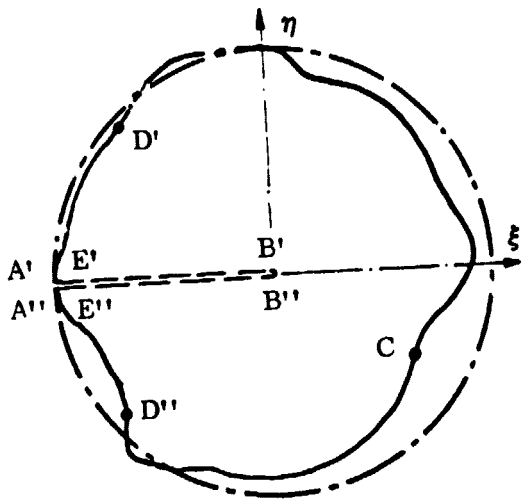

Figure 7. - Intermediate ("circle") plane used in conformal mapping sequence. Deformed circle corresponds to the realistic airfoil shape.

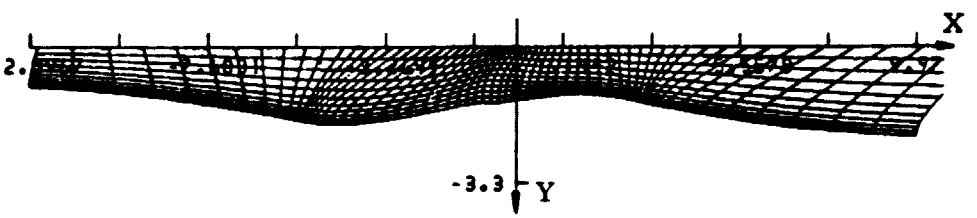

Figure 8. - "Strip" plane obtained by conformally mapping "circle" plane. Upper boundary corresponds to periodic boundaries, and lower boundary to airfoil shape.

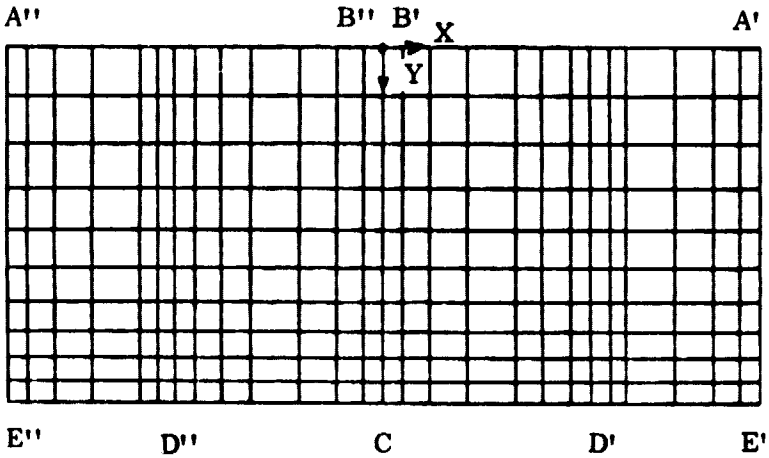

Figure 9. - Nonorthogonal coordinate shearing and stretching concept applied to X (eqs. 34, 36, and 39) and Y (eq. 38) coordinates results in a desired rectangular computational surface.

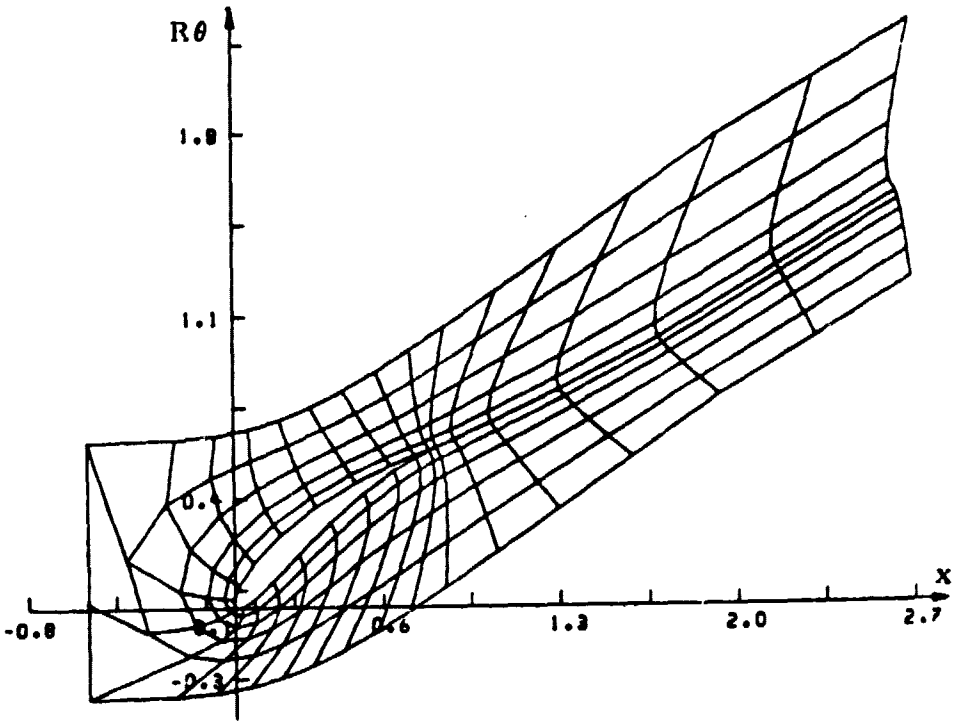

Figure 10. - An example of a two-dimensional (x,Rθ) surface discretized with a coarse, C-type, periodic grid.

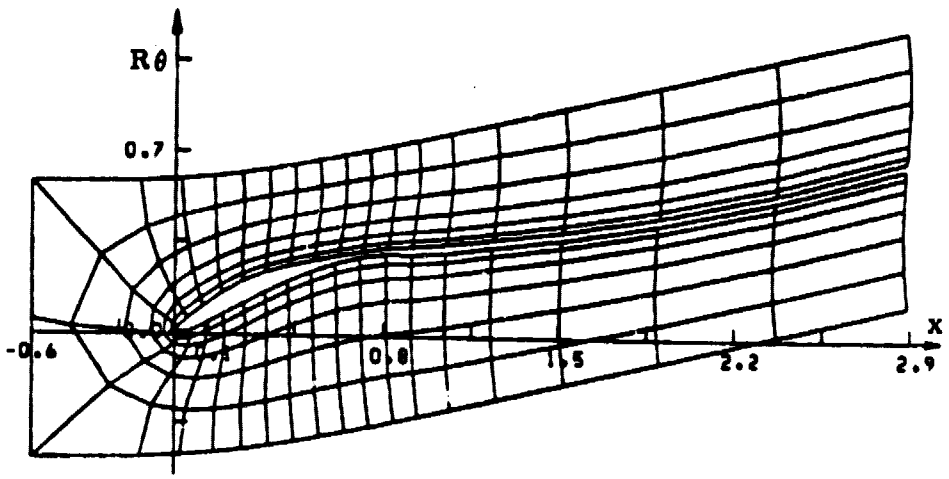

Figure 11. -- Two-dimensional (x,Rθ), C-type, periodic, boundary conforming grid for a cascade of blades with open trailing edges.

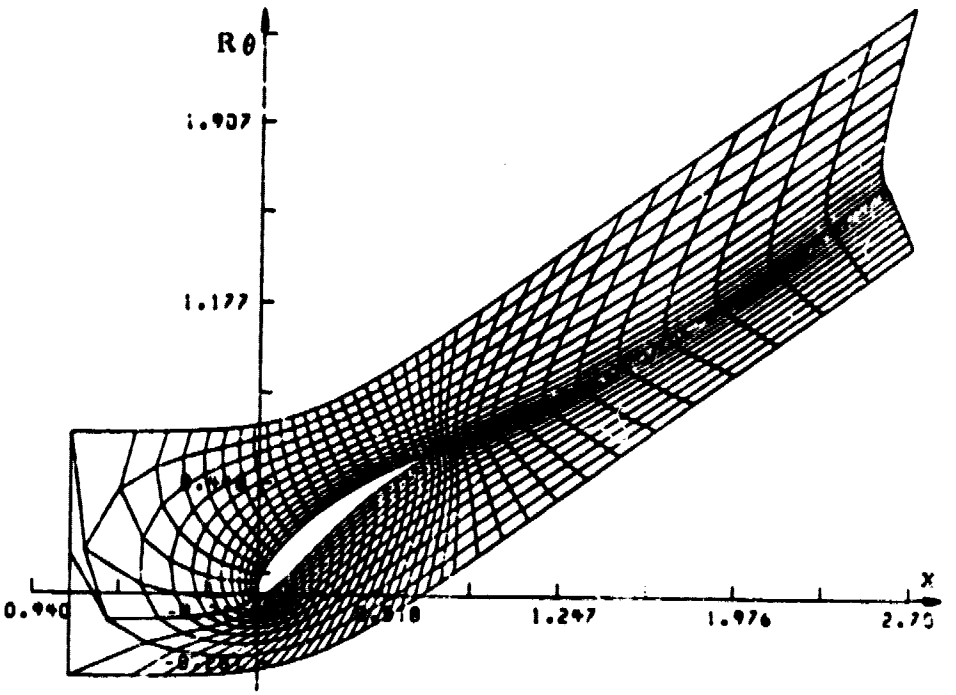

Figure 12. - Effect of controlled grid clustering. Grid points can be easily concentrated in the regions of leading and trailing edges as well as closer to the surface of the airfoil and its wake.

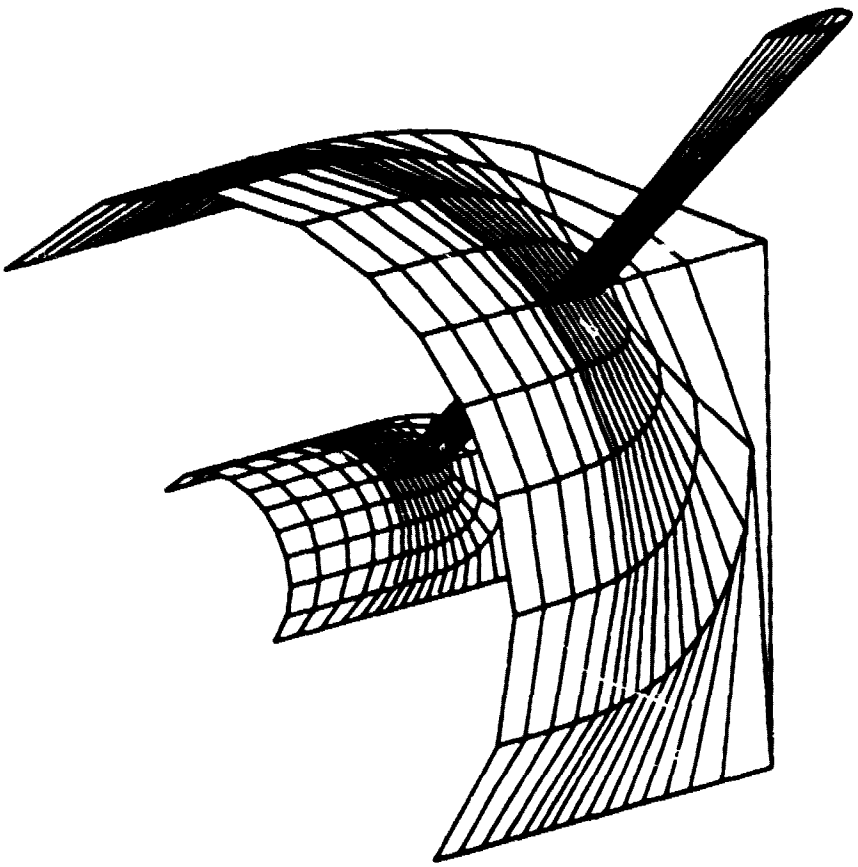

Figure 13. - Elements of a three-dimensional, C-type, periodic grid generated by GRID3C code for a geometry consisting of a rectangular unswept wing attached to a circular cylinder. Note deteriorating grid quality in the far upstream region. Only every fourth cylindrical surface is shown.

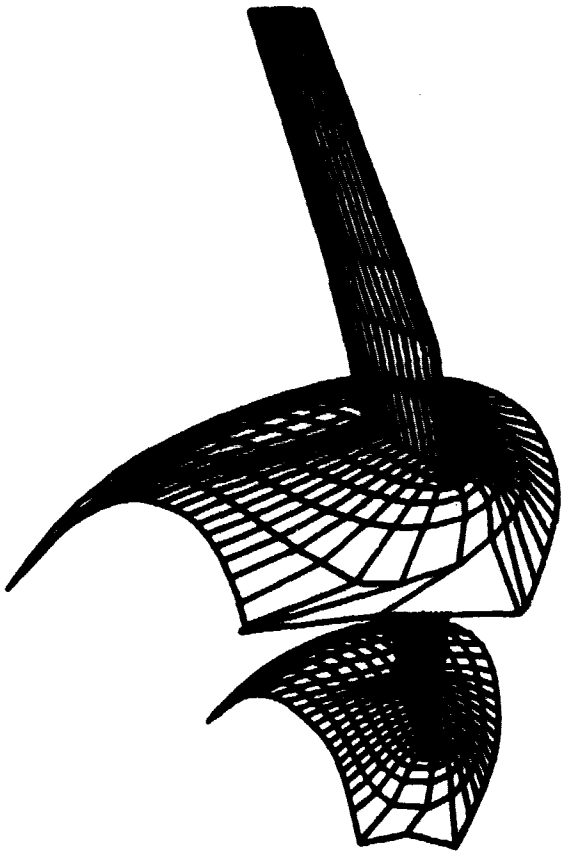

Figure 14. - Blade surface grid and one of the axisymmetric surfaces generated by GRID3C for an advanced, eight-blade NASA prop fan.

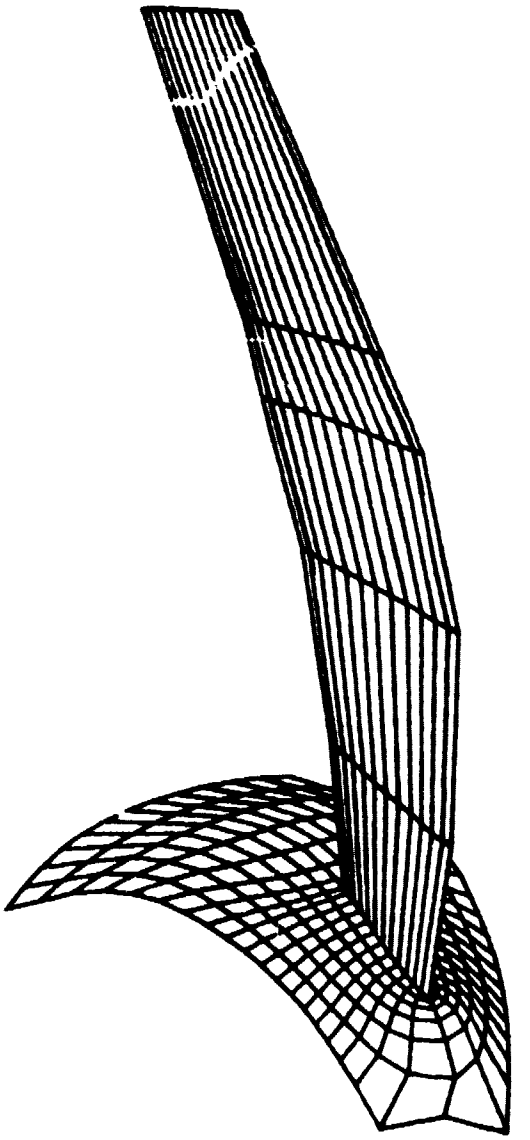

Figure 15. - Another view of the same prop fan grid generated by GRID3C shows more clearly the axisymmetric shape of the propeller hub surface.